

Sensitivity to N/Z ratio in fragment productions for the isobaric systems $^{124}\text{Xe} + ^{64}\text{Zn}$, ^{64}Ni and $^{124}\text{Sn} + ^{64}\text{Ni}$ at $E/A = 35$ MeV

E. DE FILIPPO⁽¹⁾, A. PAGANO⁽¹⁾, P. RUSSOTTO⁽¹⁾, L. ACOSTA⁽²⁾⁽³⁾,
L. AUDITORE⁽⁴⁾, V. BARAN⁽⁵⁾, T. CAP⁽⁶⁾, G. CARDELLA⁽¹⁾, M. COLONNA⁽²⁾,
D. DELL'AQUILA⁽⁷⁾, S. DE LUCA⁽⁴⁾, L. FRANCALANZA⁽⁷⁾, B. GNOFFO⁽¹⁾⁽⁸⁾,
G. LANZALONE⁽⁹⁾⁽²⁾, I. LOMBARDO⁽⁷⁾, C. MAIOLINO⁽²⁾, N. S. MARTORANA⁽¹⁰⁾⁽²⁾,
T. MINNITI⁽¹¹⁾, S. NORELLA⁽⁴⁾, E. V. PAGANO⁽¹⁰⁾⁽²⁾, M. PAPA⁽¹⁾, E. PIASECKI⁽¹²⁾,
S. PIRRONE⁽¹⁾, G. POLITI⁽¹⁰⁾⁽¹⁾, F. PORTO⁽¹⁰⁾⁽²⁾, L. QUATTROCCHI⁽¹⁰⁾⁽¹⁾,
F. RIZZO⁽¹⁰⁾⁽²⁾, E. ROSATO⁽⁷⁾[†], K. SIWEK-WILCZYŃSKA⁽¹³⁾, A. TRIFIRÒ⁽⁴⁾,
M. TRIMARCHI⁽⁴⁾, G. VERDE⁽¹⁾, M. VIGILANTE⁽⁷⁾ and J. WILCZYŃSKI⁽⁶⁾[†]

⁽¹⁾ INFN, Sezione di Catania - Catania, Italy

⁽²⁾ INFN, Laboratori Nazionali del Sud - Catania, Italy

⁽³⁾ Instituto de Física, Universidad Nacional Autónoma de México - México City, México

⁽⁴⁾ INFN, Gruppo coll. di Messina and Dip. MIFT University of Messina - Messina, Italy

⁽⁵⁾ Physics Faculty, University of Bucharest - Bucharest, Romania

⁽⁶⁾ National Center for Nuclear Research - Otwock, Poland

⁽⁷⁾ INFN, Sezione di Napoli and Dip. di Fisica, Univ. of Napoli - Napoli, Italy

⁽⁸⁾ CSFNSM - Catania, Italy

⁽⁹⁾ Università Kore - Enna, Italy

⁽¹⁰⁾ Dip. Fisica e Astronomia, University of Catania - Catania, Italy

⁽¹¹⁾ CNR, IPCF - Messina, Italy

⁽¹²⁾ University of Warsaw, Heavy Ion laboratory - Warsaw, Poland

⁽¹³⁾ University of Warsaw, Phys. Faculty - Warsaw, Poland

received 10 January 2017

Summary. — Intermediate-Mass Fragments (IMF) statistical and dynamical emission probabilities were examined in dissipative collisions of $^{124}\text{Xe} + ^{64}\text{Zn}$ and ^{64}Ni at beam energy of 35 A MeV and compared with previous studies of the $^{124}\text{Sn} + ^{64}\text{Ni}$ reaction. For these isobaric systems the probability of dynamical emission enhances with increasing of the N/Z asymmetry of the entrance channel, while the cross section of statistical emission is independent from the neutron richness of the system. Therefore, the dynamical component of the IMF emission cross section shows a strong sensitivity on the isospin of the entrance channel.

[†] Deceased.

1. – Introduction

In non-central dissipative heavy-ion collisions at the Fermi energies regime the reaction dynamics can result in the formation of a binary system of excited projectile-like (PLF) and target-like fragments (TLF). An important cross-section is also related with reactions where the PLF and TLF residues are accompanied by one or more IMFs (Intermediate-Mass Fragments) in the exit channel, generally defined as fragments with $Z \geq 3$ [1]. The emission of IMFs and light charged particles reflects the complex dynamics and different reaction mechanisms taking place during the time evolution of the reaction, while their multiplicity is principally linked to the centrality of the collision. The analysis of the reactions $^{124}\text{Sn} + ^{64}\text{Ni}$ and $^{112}\text{Sn} + ^{58}\text{Ni}$ at 35 A MeV [2] has shown that light IMFs ($Z \leq 9$) are preferentially emitted at mid-rapidity in the neck fragmentation channel and produced either on short times scales (prompt neck rupture emission) or on longer ones in the sequential decay of the PLF or TLF primary fragments. Emission of heavier IMFs ($Z > 9$) is found to appear at a later stage of the neck expansion process and it is dominated by an asymmetric mass splitting of the PLF in a aligned break-up configuration (“dynamical fission”) [3, 4] or by a sequential statistical decay of the PLF. This last decay pattern is isotropic in the reference frame of the PLF source and it happens at longer time scales [3, 5].

Many experimental observations have shown that the isotopic composition N/Z of the IMFs fragments originating from neck fragmentation is enriched in neutrons as compared with expectation of the statistical decay [6]. Comparisons with transport models have provided that the neutron to proton ratio of the IMFs emitted in the neutron rich neck region is sensitive to the symmetry term of the nuclear equation of state (EOS) at low barionic density below ρ_0 [2]. On the other hand, in the range of energies from above the Coulomb barrier up to Fermi ones, to what extent the isospin asymmetry of the entrance channel influences the dynamics of the collision is less clearly understood: i) stochastic mean-field calculations (SMF) show that the competition between binary splitting and ternary break-up is influenced by the stiffness of the symmetry energy in neutron rich nuclei [7]; ii) in nuclear reactions involving projectile calcium isotopes at 25 A MeV it was shown that the competition between heavy-residue production *vs.* binary break-up can be attributed to the difference in the neutron-to-proton ratio of the entrance channels [8]; iii) for the reaction $^{124}\text{Sn} + ^{64}\text{Ni}$ and $^{112}\text{Sn} + ^{58}\text{Ni}$ at 35 A MeV, it was shown that, while the statistical emission gives the same cross section for the two systems as a function of the IMF atomic number of the emitted fragments, the dynamical IMF emission cross section is enhanced by a factor ranging between 1.5–2 for the neutron-rich system, therefore evidencing a strong sensitivity to the isospin of the entrance channel [3, 9].

The object of the present work is a new experimental investigation, named InKiIsSy (Inverse Kinematic Isobaric Systems), aimed to study at the same incident beam energy of 35 A MeV, the binary splitting of the PLF in the two isobaric systems $^{124}\text{Xe} + ^{64}\text{Zn}$, ^{64}Ni , to be compared with the previous studies of the $^{124}\text{Sn} + ^{64}\text{Ni}$ reaction [9]. The main goal is to pin down genuine entrance channel isospin effects by comparing isotopic systems of different isospin.

2. – Experimental results

The experiment was performed at the LNS cyclotron facility in Catania by using the ^{124}Xe beam at 35 A MeV incident on targets of ^{64}Zn ($308 \mu\text{g}/\text{cm}^2$) and ^{64}Ni ($370 \mu\text{g}/\text{cm}^2$). Charged reaction products were detected with the 4π CHIMERA detector coupled to a

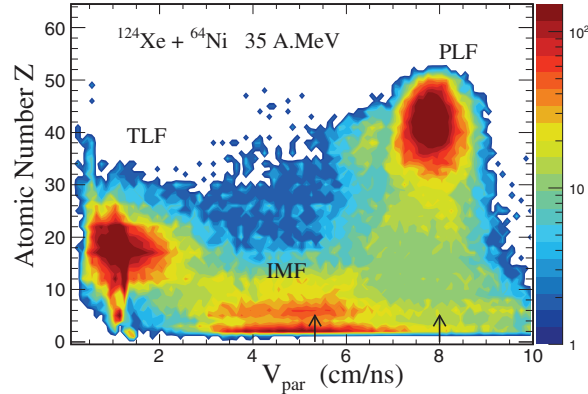


Fig. 1. – In the reaction $^{124}\text{Xe} + ^{64}\text{Ni}$, atomic numbers Z of particles in a given event are displayed as a function of their longitudinal velocities V_{par} along the beam axis.

prototype of the FARCOS [10] correlator array (four telescopes), placed at 25 cm from the target and subtending the polar angles of $15^\circ \leq \theta_{lab} \leq 45^\circ$ and the azimuthal interval $\Delta\phi \approx 90^\circ$. This device was used to measure with better angular and energy resolution than in CHIMERA, IMF-IMF and p - p correlations. The analysis shown in the following is only limited to particles identified in the CHIMERA array.

Particles punching-through the Silicon detectors, in the CHIMERA Si-CsI telescopes, were identified in charge (and mass for light ions, $Z < 9$) by using the ΔE - E technique; light charged particles ($Z \leq 3$) were isotopically identified in CsI(Tl) scintillators. For particles stopping in the silicon detectors mass identification is performed by using the Time-of-Flight (TOF) with respect to the high frequency timing signal of the cyclotron pulsed beam. Finally particles stopped in silicon detectors were also identified in charge (up to $Z < 20$ and for $\theta > 7^\circ$) by means of a pulse shape technique based on signal rise time measurement as a function of the particles energy [11]. In fig. 1 the particles atomic numbers are plotted *vs.* their longitudinal velocities V_{par} along the beam axis with a minimum selection of events where the total particles longitudinal detected linear momentum is equal to at least 60% of the projectile one. The figure shows well the regions of PLF, TLF and IMFs located around the center of mass velocity. In order to study the main features of the PLF break-up, we selected events for which $Z_{2F} = Z_H + Z_L > 30$, being Z_H and Z_L the two biggest fragments in the event, with masses equal respectively to A_H and A_L (heavy and light one). We show in fig. 2, for the reaction $^{124}\text{Xe} + ^{64}\text{Ni}$, the distribution of Z_{2F} as a function of the parallel velocity of the lighter fragment. Plots are reported for two windows of the total kinetic energy, $E_{2F} = E_H + E_L$, (left and right columns, respectively) of the two fragments (higher values indicate less dissipative collisions) and from top to bottom for increasing values of the mass asymmetry of the two fragments.

We observe that for $V_{par}^{LIGHT} \geq 3$ cm/ns the light fragment velocity presents two components characteristic of “forward” and “backward” emission in the PLF source frame: the scattering of the PLF is followed by its splitting into two fragments [3, 5]. For $V_{par}^{LIGHT} < 3$ cm/ns we note also a further component that clearly can be interpreted as a target remnant. The yield of the PLF backward component increases with the mass asymmetry A_H/A_L and for the most dissipative collisions. The scenario of the

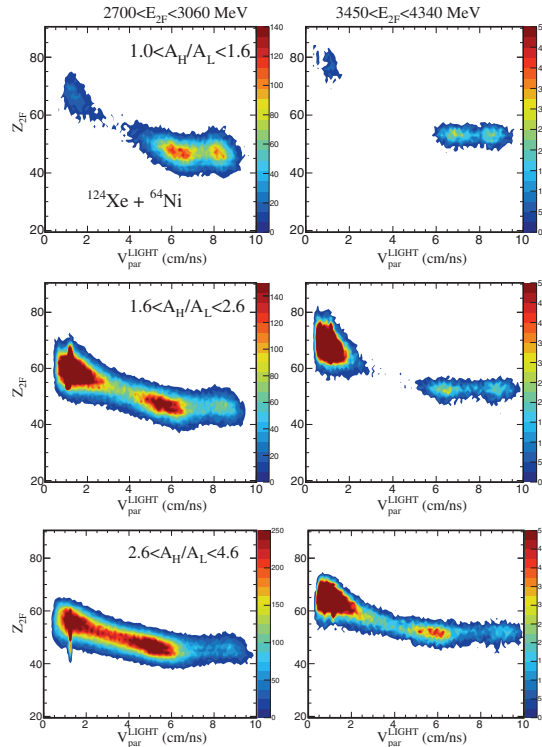


Fig. 2. – In the reaction $^{124}\text{Xe} + ^{64}\text{Ni}$, the distribution of the sum of charges of two heaviest fragments (Z_{2F}) is plotted as a function of longitudinal velocities V_{par} of the lighter fragment for two different windows of the total fragments kinetic energy and, from top to bottom, for growing mass asymmetries A_H/A_L ratio.

PLF break-up is better seen in fig. 3 where the V_{par} *vs.* the V_{per} Galilean invariant cross section is drawn for the lighter fragment in the PLF source reference frame for $2700 < E_{2F} < 3060$ MeV. The left panel, collecting the most asymmetric splittings ($2.6 < A_H/A_L < 4.6$), shows clearly a forward-backward asymmetry where the light fragments are prevalently backward emitted between their heavy PLF partner and the TLF, in an aligned configuration that characterizes the so called “dynamical fission”. Conversely, in the right panel for symmetric splitting, we observe the typical pattern of a forward-backward symmetry around a well defined Coulomb ring: this last is what is expected for a sequential, equilibrated break-up.

In fig. 4 we show, for the two reactions $^{124}\text{Xe} + ^{64}\text{Ni}$ and $^{124}\text{Xe} + ^{64}\text{Zn}$ the distribution of $\cos(\theta_{prox})$, where θ_{prox} is defined as the angle between the PLF source flight direction (measured in the center of mass of the reaction) and the relative velocity between Z_H and Z_L fragments. The spectra in the figure have been constructed with conditions for asymmetric mass splitting ($2.6 < A_H/A_L < 4.6$) and less dissipative collisions ($3450 < E_{2F} < 4340$ MeV) and with further conditions on $V_{rel}(\text{PLF}, \text{IMF})$ [9] in order to reject the target remnants. The distribution results from the superposition of a symmetric component and a pronounced peak $\cos(\theta_{prox}) \approx 1$, corresponding to a backward emission of the fragment, aligned along the direction of the PLF. This anisotropy is one signature

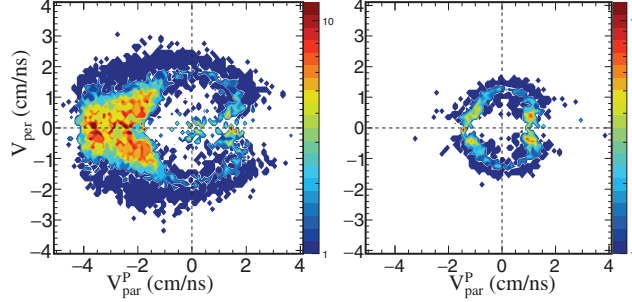


Fig. 3. – For the reaction $^{124}\text{Xe} + ^{64}\text{Ni}$, invariant cross section for the lighter fragment in the reference frame of the PLF source for $2.6 < A_H/A_L < 4.6$ (left panel) and $1 < A_H/A_L < 1.6$ (right panel).

of a “dynamical” process [2, 9, 12]. It is important to note, comparing the two spectra for different targets, that this dynamical component is enhanced for the reaction with a neutron-rich target, ^{64}Ni with respect to the ^{64}Zn one.

In order to evaluate and separate quantitatively the dynamical and statistical component emissions as a function of the charge of the emitted fragments, we have applied the methods described in ref. [9, 13] that use the $\cos(\theta_{prox})$ as main observable. The most important points of this analysis are: i) the selections of events in which the IMF multiplicity M_{IMF} is strictly equal to one; ii) the rejection of events in which IMFs originates from TLFs fragmentation or decay; iii) the dynamical component is obtained subtracting from the total $\cos(\theta_{prox})$ distribution, the portion of angular distribution that is symmetric around $\cos(\theta_{prox}) = 0$.

In fig. 5 we present the ratio of the dynamical component with respect to the dynamical+statistical one for the two systems $^{124}\text{Xe} + ^{64}\text{Ni}$ and $^{124}\text{Xe} + ^{64}\text{Zn}$. Results show clearly that the dynamical component is greater (for $Z_{IMF} > 7$) for the reaction with a neutron rich target (^{64}Ni). Careful complete comparison of these data with the other

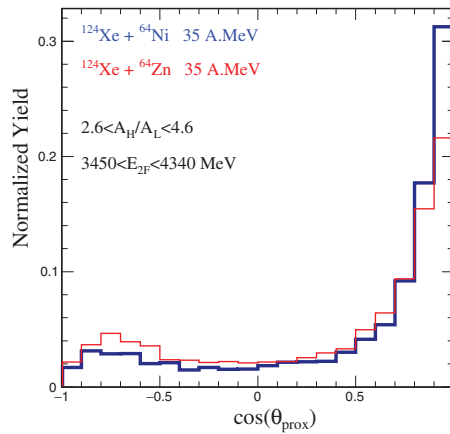


Fig. 4. – Comparison of $\cos(\theta_{prox})$ distributions for the two reactions $^{124}\text{Xe} + ^{64}\text{Ni}$ (thick blue line) and $^{124}\text{Xe} + ^{64}\text{Zn}$ (thin red line).

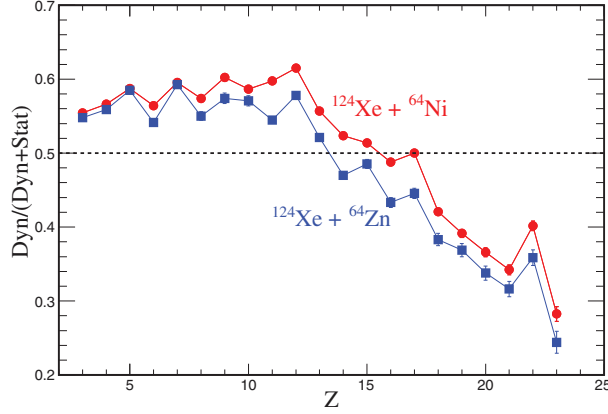


Fig. 5. – Ratio of the dynamical component *vs.* the total (statistical+dynamical) as a function of the IMF atomic number for the $^{124}\text{Xe} + ^{64}\text{Ni}$ (red circles) and $^{124}\text{Xe} + ^{64}\text{Zn}$ (blue squares) reactions.

isobaric system $^{124}\text{Sn} + ^{64}\text{Ni}$ previously studied, will be presented in a forthcoming paper [14]. Results confirm the scaling of the dynamical component in the IMF's emission with the isospin of the entrance channel for a wide charge range of IMF's fragments. Due to the use of isobaric systems, independence of the results from the size of the projectile and target is also indicated.

In fig. 6 we present a comparison of the experimental data of fig. 5 for the reaction $^{124}\text{Xe} + ^{64}\text{Ni}$ with a preliminary simulation in the frame of the constrained molecular dynamics, CoMD-III, code [15]. CoMD was already used to describe the gross features of dynamical emission phenomena in $^{124}\text{Sn} + ^{64}\text{Ni}$ reaction at 35 A MeV [16].

In this calculation code parameters were not varied. The $^{124}\text{Xe} + ^{64}\text{Ni}$ was simulated up to 650 fm/c. After which the GEMINI code [17] was used for statistical de-excitation of hot particles. The theoretical data were analyzed as the experimental ones in order

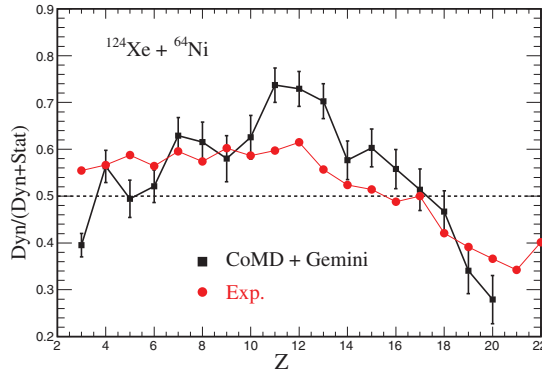


Fig. 6. – For the $^{124}\text{Xe} + ^{64}\text{Ni}$ reaction, ratio of the dynamical component *vs.* the total (statistical+dynamical) as a function of the IMF atomic number experimental data (red circles) and results of CoMD3+GEMINI theoretical (black squares) calculations. (Preliminary results).

to obtain the theoretical ratio of the dynamical component *vs.* the total (statistical + dynamical) in PLF break-up, but no detectors setup filter was applied. Despite these limitations the data comparison in the fig. 6 seems very promising. It is interesting to note that the CoMD model gives also the possibility to vary the isospin-dependent part of the interaction in order to provide different parametrizations of the symmetry energy component of the EOS [8, 18, 19].

In conclusion we have evaluated the probability for dynamical and statistical emission in collisions of ^{124}Xe with ^{64}Ni and ^{64}Zn targets at 35 A MeV. For these isobaric systems we have shown that the probability of dynamical IMF's emission is greater when using the neutron rich ^{64}Ni target, evidencing a strong sensitivity to the isospin of the entrance channel. The dynamical IMF emission is an important mechanism to constrain the density dependence of the symmetry energy but this needs calculations that are able to follow the largest reaction time-scales of the IMF emission. For this reason we have started transport model calculations by using the CoMD model. In the future we want to extend these studies at lower beam incident energy in the transition energy region from Coulomb to Fermi energies around 20 A MeV with stable beams and at lower energies (< 15 A MeV) with future radioactive beams at SPES [20, 21].

REFERENCES

- [1] DAVIN B. *et al.*, *Phys. Rev. C*, **65** (2002) 064614.
- [2] DE FILIPPO E. *et al.*, *Phys. Rev. C*, **86** (2012) 014610.
- [3] RUSSOTTO P. *et al.*, *Phys. Rev. C*, **81** (2010) 064605.
- [4] MCINTOSH A. B. *et al.*, *Phys. Rev. C*, **81** (2010) 034603.
- [5] DE FILIPPO E. *et al.*, *Phys. Rev. C*, **71** (2005) 064604.
- [6] DE FILIPPO E. and PAGANO A., *Eur. Phys. J. A*, **50** (2014) 32, and references therein.
- [7] BARAN V. *et al.*, *Phys. Rep.*, **410** (2005) 335.
- [8] CARDELLA G. *et al.*, *Phys. Rev. C*, **85** (2012) 064609.
- [9] RUSSOTTO P. *et al.*, *Phys. Rev. C*, **91** (2015) 014610.
- [10] PAGANO E. V. *et al.*, *EPJ Web of Conferences*, **117** (2016) 10008.
- [11] ALDERIGHI M. *et al.*, *IEEE Trans. Nucl. Sci.*, **52** (2005) 1624.
- [12] HUDAN S. *et al.*, *Phys. Rev. C*, **86** (2012) 021603.
- [13] BOCAGE F. *et al.*, *Nucl. Phys. A*, **676** (2000) 391.
- [14] RUSSOTTO P. *et al.*, in preparation.
- [15] PAPA M., *Phys. Rev. C*, **87** (2013) 014001.
- [16] PAPA M. *et al.*, *Phys. Rev. C*, **75** (2007) 054616.
- [17] CHARITY R. J. *et al.*, *Phys. Rev. C*, **82** (2010) 014610.
- [18] STIEFEL K. *et al.*, *Phys. Rev. C*, **90** (2014) 061605.
- [19] CAMMARATA P. *et al.*, *Nucl. Instrum. Methods A*, **761** (2014) 1.
- [20] NEWCHIM COLLABORATION, SPES Letter Of Intent (2016).
- [21] RIZZO C. *et al.*, *Phys. Rev. C*, **90** (2014) 054618.